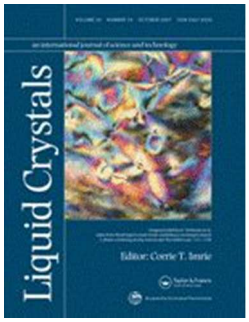

Characterization of polymerization-induced phase separation process in polymer dispersed liquid crystals based in hydroxyalquil-methacrylate matrices

Journal:	*Liquid Crystals*
Manuscript ID	Draft
Manuscript Type:	Original Article
Date Submitted by the Author:	n/a
Complete List of Authors:	Hegoburu, Ignacio; INTEMA Soule, ezequiel; INTEMA,
Keywords:	polymer-dispersed liquid crystal, photo-polymerization, polymerization kinetics, morphologies, polymerization-induced phase separation

Characterization of polymerization-induced phase separation process in polymer dispersed liquid crystals based in hydroxyalquil-methacrylate matrices

Ignacio Hegoburu, Ezequiel Rodolfo Soulé*

Nanostructured Polymers, Institute of Materials Science (INTEMA), University of Mar del Plata – National Research Council, Mar del Plata, Argentina.

*corresponding author: ersoule@fi.mdp.edu.ar

Characterization of polymerization-induced phase separation process in polymer dispersed liquid crystals based in hydroxyalquil-methacrylate matrices

Hydroxyalquil methacrylates are very well known hydrogel-forming biocompatible polymers. In this work, polymer-dispersed liquid crystals based in hydroxyethyl- and hydroxypropyl methacrylate (HEMA and HPMA) matrices are synthesized and characterized. Two different liquid crystals from the cyano-biphenyl family (5CB and 8CB) are used. Polymerization kinetics, phase transitions, and morphologies generated in the polymerization-induced phase separation process are analyzed. It is found that phase separation is produced at very low conversions, producing initially the segregation of a polymer-rich phase. Due to the auto-acceleration effect of free-radical polymerizations, this produces an increase in the low-conversion polymerization rate. The liquid crystalline transition temperature decreases as the concentration of liquid crystal (LC) decreases, indicating that this phase is impurified. 8CB is found to be less miscible than 5CB with the matrices, so the LC-rich phase for 5CB is more impurified and its total volume in the material is smaller.

Keywords: polymer-dispersed liquid crystal; photo-polymerization; polymerization kinetics, morphologies, polymerization-induced phase separation

1. Introduction

Polymer-dispersed liquid crystals (PDLCs) are functional composite materials consisting of droplets of liquid crystalline phase dispersed in an isotropic polymer. These functional materials are used in electro-optical applications such as switchable windows, displays, spatial light modulators, tunable filters, and other devices[1–4]. PDLC materials can also be thermally actuated to transition from opaque to transparent states[5], allowing for other types of applications such as thermal sensors and active elements in thermo-optical memory devices. The optical transitions are characteristic of liquid crystalline phases, also called mesophases, due to the dependence of the difraction index on the degree of ordering, and on the relative directions of molecular

alignment, light incidence and polarization.

The standard approach to producing PDLCs is polymerization-induced phase separation (PIPS)[3–8]. The monomer is polymerized in a mixture with the liquid crystal (LC). If the LC is miscible with the monomer but not with the polymer, a phase separation is produced during the polymerization. Photo-polymerization is usually preferred due to the fast curing speed, uniformity, and ease of controlling the reaction (through irradiation intensity and time). In addition, photo-polymerization can be performed at room temperature.

Lately, there has been interest in the characterization of PDLCs based in bio-compatible matrices, for possible biomedical and bioengineering applications. Different matrices have been studies such as chitosan[9], polyvinyl alcohol boric acid[10,11], polysulfone[12], or hydrogel-forming polyacrylamide[13]. One possible biomedical application of bio-compatible PDLC could be as artificial irises, constructed as an array of concentric rings that can be individually actuated[14], thus, the central rings are in a transparent state and the outer states become opaque as a function of light intensity, similar to natural irises.

Polymer matrices based in hydroxyethyl- and hydroxypropyl-methacrylate (HEMA and HPMA), are biocompatible materials, due to their ability of absorbing water and forming hydrogels. Their main uses (specially HEMA) are in dental [15,16], and ophthalmic applications[17–21]. HEMA is a base material for modern contact lenses and hydrophilic acrylic intraocular lenses (usually they are made of copolymers of HEMA). As such, these matrices can be candidates for the construction of PDLC-based artificial irises, for example. Due to the high concentration of hydroxyl groups in these polymers, strong specific interactions (hydrogen bonds) exist, so a very low

miscibility with most LC is expected (except if the can form hydrogen bonds too), which will result in very low phase-separation conversions.

In this work, PDLCs based in alkyl-cyanobiphenyl liquid crystals, dispersed in poly-HEMA and HPMA matrices are studied. The materials are synthesized by photo-PIPS, and the polymerization kinetics, phase behaviour and morphologies are characterized. In section 2 the materials and experimental techniques are described. Section 3 shows the main results, describing the reaction kinetics of different combinations of monomers/LC with different compositions, the mesophase transition temperatures, and the morphologies; here a qualitative phase diagram is constructed from all the previous observed behaviour. Finally the last section presents the main conclusions.

2. Materials and methods

2.1 Materials

The LCs 4'-penyl-4-cyanobiphenyl (5CB) and 4'-octyl-4-cyanobiphenyl (8CB) were purchased from Synthon Chemicals and used as received. 5CB can exist in crystalline (Cr), nematic (N), and isotropic (I) phases, with the following transition temperatures: $T_{Cr\text{-}N}$=23.7°C and $T_{Cr\text{-}N}$=35.3°C. 8CB, in addition to Cr and N phases, shows a stable smectic (Sm) phase, with the following transition temperatures: $T_{Cr\text{-}Sm}$=21.4°C, $T_{Sm\text{-}N}$=33.4°C and $T_{N\text{-}I}$=40°C.

Hydroxyethyl methacrylate (HEMA) and hydroxypropyl methacrylate (HPMA) were purchased from Sigma-Aldrich and used as received. Camphorquinone and ethyl-4-dimethylaminobenzoate were used as initiators for photo-polymerization (1%wt each, relative to monomer mass).

2.2 Sample Preparation.

First, camphorquinone and ethyl-benzoate were dissolved in the monomer and then the monomer-initiator mixture was mixed with the LCs. The mixture was sandwiched between two glass plates. The thickness of the film was adjusted to 5 μm by using silica bead spacers (200 microspheres/mm^2), or (for SEM samples) to 60 μm with a polyethylene tape. The mixture was irradiated for different periods of time (as indicated in each case) with a blue LED lamp, built in our laboratory, with a wavelength range of 410–530 nm and light irradiance of 130 mW/cm^2.

2.3 Polymerization kinetics.

Samples were illuminated for intervals of 5 seconds, and a Fourier-Transform-Infrared (FTIR) spectrum was taken in a Matson Genesys II apparatus after each illumination period. The area of the absorption band located at 1640 cm^{-1} (C=C bond), relative to that 3300 cm^{-1} (OH group), was used to calculate the C=C conversion. As dark polymerization can take place in photo-polymerizing systems, some runs were performed with longer irradiation intervals in order to assess the effect of dark-polymerization between irradiation intervals. In addition, some samples were left after irradiation at room temperature, in the dark or exposed to ambient light, and FTIR spectra were taken at different times.

2.4. DSC Measurements.

DSC measurements were performed on a Perkin-Elmer Pyris 1 apparatus equipped with a Perkin-Elmer 2P intracooler, using a few milligrams of cured materials. A heating ramp of 10 °C/min was used in the temperature range spanning from 0 to 60 °C. Two runs were performed per sample, and the data were analyzed in the second run.

2.5. Optical Microscope Measurements.

A Leica DMLB microscope equipped with a video camera (Leica DC100) and a hot stage (Linkam THMS 600) was used. Samples were heated above TNI, and then they were cooled and left for a few minutes at different temperatures until the formation of the nematic phase was observed (with crossed polarizers). Then the sample was heated until the nematic phase disappeared. The process was repeated until the transition temperature was located within a 1ºC interval.

2.5. Scanning electron microscopy.

60 μm thick films where prepared and then fractured, and the fracture surface was observed by scanning electron microscopy (SEM) on a Jeol JSM 35 CF device.

3. Results and discussion

3.1 Polymerization kinetics

The reaction kinetics was followed, as described in the experimental section, by irradiating a sample in intervals of 5 seconds, and taking FTIR spectra between irradiations. This methodology is very convenient as a single sample can be used to follow the entire polymerization, but it introduces some error due to dark polymerization, and to possible exposition to ambient light between irradiation periods. FTIR of samples were taken after irradiating the sample leaving it in dark for some time; no significant reaction advance was observed in samples with low initial conversion, while the samples with initial intermediate conversion (>0.5), showed some degree of dark polymerization. This was independent of the LC content of the sample. Attempts were made to follow the kinetics by using samples under continuous irradiation; that is, preparing several films, irradiating them for different times, and

measuring each conversion. Although this should minimize dark-polymerization effects, it introduces an important scattering in the conversion data (ascribed to the fact that each measurement correspond to a different sample). It was observed that the shape of the curve is qualitatively similar in the case of continuous-irradiation and interval-irradiation, in the latter case just an apparent faster kinetics is observed.

Figure 1 shows the kinetics of polymerization for HEMA (using interval irradiation), pure and with different amounts of 8CB. High conversion (>90%) is attained for all materials within few minutes. HEMA photo-polymerization initiated by DMPA at 30 ºC has been studied in the literature[22] and the reported conversion-time curve is qualitatively similar to that shown in figure 1.

In the case of pure HEMA as well as with 10% of LC, an auto-acceleration at intermediate conversion can be clearly seen. This is a very well known effect in free-radical polymerizations and it has been observed in HEMA photo-polymerization[22]. The bimolecular termination reaction becomes strongly limited by diffusion at much lower conversions than propagation or initiation, which leads to an increase in the global reaction rate. This is due to the fact that bimolecular termination involves two polymeric molecules, which are much more affected by mobility limitations than monomer or initiator species. As the polymer concentration increases, both the decrease in free volume and the increase in chain entanglements impose strong limitation to macromolecular diffusion, leading to the decrease in termination rate.

It is noted that the observed auto-acceleration could be exaggerated due to dark-polymerization effects (which, as explained, are more important at intermediate-high conversions). Nevertheless, as explained before, the shape of the conversion-time curve is similar for interval and continuous irradiation, and it is also similar to the one

reported in the literature[22]. In addition, auto-acceleration is not observed for high LC content (while on the other hand, dark polymerization was observed).

An interesting observation is that, for low conversions, the addition of LC increases the reaction rate, while for high conversions the kinetics is clearly slowed down. This can be ascribed to an early phase separation (see next sections), which generates a polymer-rich phase. Within this phase, as the polymer concentration is high, the reaction is accelerated, leading to a higher average reaction rate. Later on, as monomer is depleted in this phase, the reaction continues in the LC-rich, polymer poor phase, at a slow rate. The polymer concentration in the polymer-rich phase is higher for higher LC- contents, so the global reaction is faster. But, as the maximum volume of polymer-rich will be smaller, and in addition the polymer concentration is closer to the concentration of maximum reaction rate, the sigmoid shape in the conversion-time curve is not observed.

Figure 2 shows the reaction rate for the four materials with 50% LC content: HEMA/8CB, HEMA/5CB, HPMA/8CB, HPMA/5CB. The kinetics of HPMA polymerization with both types of LC are very similar, whereas for the case of HEMA, the kinetics is more strongly dependent of the LC. It is difficult to extract a consistent trend as some of the curves intersect each other at intermediate conversions. But focusing in the low conversion region, it can be observed that the polymerization rate is higher for materials with HEMA than with HPMA, and with 5CB than with 8CB. It is worth to mention that no significant difference was observed in the polymerization rates of pure HEMA and pure HPMA in the whole conversion range, so the differences observed in the mixtures of LC are expected to be produced by the effects of phase separation. According to the observed low-conversions reaction rates and the explanation introduced in the previous paragraph, it is expected that the polymer

concentration in the polymer-rich phase, or/and the volume of this phase, is higher for 5CB than for 8CB, and for HEMA than for HPMA.

3.2 Phase Transitions

Monomers are miscible with the LCs up to very high LC contents (for high enough LC contents, nematic-isotropic coexistence is expected at room temperature). Polymers, on the other hand, are highly immiscible: isotropic-nematic coexistence is observed in for LC content >10%, and isotropic-isotropic coexistence is observed upon heating the system up to 120ºC.

During polymerization, phase separation is observed at very low conversion (less than 5 seconds of irradiation), as the material turns opaque. As mentioned above, a few minutes are enough for the material to reach relatively high conversions. Nevertheless, it was found that the final properties of the materials are very sensitive to small amounts of unreacted monomer. Specifically, the final value of T_{NI} (hereafter referred as $T_{NI,\infty}$), is reached after 30 minutes of irradiation, while for 15 minutes of irradiation (conversion of about 0.95), T_{NI} is several degrees Celsius below $T_{NI,\infty}$.

Figure 3 shows some POM micrographs of the material Poly-HEMA - 30%wt 8CB, at different temperatures. At low temperatures, the LC domains are fully liquid crystalline (smectic and nematic phases could not be distinguished from POM images). The transition from nematic to isotropic is not abrupt, but it takes place in a range of temperature. Although it is difficult to see it in an optical micrograph, mesophase domains seems to be of irregular shape. Figure 4 shows a DSC thermogram. Three transitions can be observed as temperature is increased: crystal-smectic, smectic-nematic, and nematic-isotropic. Note that the heat of transition is the largest for crystal melting and the smallest for the transition between the two mesophases.

Figure 5 shows $T_{NI,\infty}$ for different materials. It is observed that, for all systems, it increases with LC content and it approaches the value of T_{NI} for the pure LC ($T_{NI,LC}$), but even for 50%wt LC it is still a few degrees lower. This indicates that the LC phase is impurified (with un-reacted monomer, initiator derivatives, or short polymer chains), and that this impurification is higher for smaller LC content. Note that the value of $\Delta T_{NI}=T_{NI,LC} - T_{NI,\infty}$, is an indicative of how impurified is the LC phase, but no direct conclusion can be extracted regarding the solubility of LC in the polymer-rich phase. The meassured ΔT_{NI} for PDLCs with 8CB is always smaller than for 5CB, which indicates that the LC-rich phase has a higher purity in 8CB materials.

As mentioned before, when materials are irradiated for 15 minutes, although a high conversion is reached, T_{NI} is significantly lower than $T_{NI,\infty}$. But it was observed that, when the material is stored at room temperature, in dark, T_{NI} increases with time, eventually reaching $T_{NI,\infty}$. This "ageing" effect is ascribed to dark polymerization. At high conversions where the diffusion limitations are most important, termination is expected to very slow; consequently, although with a very slow kinetics, conversion can increase significantly in-dark, and eventually full conversion is approached and $T_{NI,\infty}$ is reached after a period of a few days. This ageing is shown for a Poly-HEMA - 50%wt 8CB material, stored in dark, after irradiation for 15 minutes, in figure 6.

3.3 Phase coexistence and morphology

Figure 7 shows SEM micrographs of different materials. A "polymer ball" morphology is observed in all cases. This morphology is generated when the polymer is strongly segregated from the monomer-LC mixture, so phase separation produces initially a polymer-rich dispersed phase. These polymer domains usually percolate at some point, forming a continuous phase and leaving the LC phase confined to the cavities within. This initial segregation of a polymer-rich phase is consistent with the

increase of reaction rate at low conversions produced by the addition of LC as explained in section 3.1 (this obviously requires that this polymer-rich phase still has a significant amount of monomer to react).

The size of the polymer domains is similar for all the materials, in the range of 1 to 3 microns. As the LC content increases, the number of polymer domains decreases, as expected. The total volume of polymer domains observed in the micrographs for materials with 50% is higher for 5CB than for 8CB, while it is similar for both matrices (it seems to be slightly higher for HEMA than for HPMA). As the LC-phase is relatively pure in all cases, and considering the lever rule, higher volume of polymer-rich phase implies higher concentration of LC in that phase, this indicates that 5CB solubility in the polymers, although small, is higher than for 8CB (this could be expected due to its lower molecular volume which favours entropy of mixing). But note that, according to the kinetic data, the polymer-rich phase is expected to have a higher polymer concentration in 5CB systems when phase separation is produced (obviously this reverts at high conversions in order for that phase to have a higher LC content at complete conversion). This requires that the tie lines have a different slope for 5CB and 8CB systems. Figure 8 shows a qualitatively phase diagram showing this situation. This kind of system, consisting in a polymer, a solvent and a non-solvent, has been studied in the literature [23,24]. 5CB is expected to be more miscible both with the polymer and the monomer (due to its smaller size, as explained before), both factors have the effect that LC distributes more evenly in the two phases (tie lines more parallel to the M-P axis). On the other hand, 8CB is less miscible with both, this makes the LC concentration in the LC-rich phase to be higher (tie lines more parallel to the LC-monomer axis, the extreme case would be that the all the tie lines converges to LC-

vertex). This is also consistent with the fact that LC-rich phase is less impurified for 8CB than 5CB, as mentioned in the previous section.

4. Conclusions

PDLCs based in two different cyano-biphenyl LCs and two hydroxyalkyl methacrylate matrices were synthesized via photo-polymerization-induced phase separation, and its polymerization kinetics, phase behaviour and morphologies were characterized. The polymer and the LCs are found be immiscible in a wide composition range up to temperatures of at least 120°C, this high incompatibility leads to a very low phase-separation conversion in the PIPS process. The reaction kinetics shows the characteristic auto-acceleration effect, commonly observed in free-radical polymerizations. The materials have a polymer-ball morphology, indicating that when phase separation is produced, a polymer-rich phase is initially segregated. As auto-acceleration arises at high polymer concentration, the formation of a polymer-rich phase increases the overall rate of polymerization, consequently the low-conversion polymerization rate increases with increasing LC content.

It was observed that the LC-rich phase has a small amount of impurities, leading to a value of TNI lower than the corresponding to the pure LC. This difference was larger for materials with 5CB, indicating a lower purity of the LC phase. In addition, from the morphologies, it was observed that the volume of the polymer rich phase is larger for materials with 5CB, indicating that the LC content in this phase is higher. From these observations and the trends observed in the rate of polymerization, schematic qualitative phase diagrams were constructed. The size of the phase coexistence regions and the slope of the tie lines are schematized according to the experimental observation, and they are consistent with 5CB being more compatible both

with the polymers and the monomers than 8CB (as expected due to the more favourable entropy of mixing of smaller molecules).

Acknowledgements

Funding from the National Agency for Promotion of Science and Technology (ANPCyT), and University of Mar del Plata (UNMdP) is gratefully acknowledged.

References

[1] Büyüktanir E a., Mitrokhin M, Holter B, et al. Flexible Bistable Smectic-A Polymer Dispersed Liquid Crystal Display. Jpn. J. Appl. Phys. 2006;45:4146–4151.

[2] Date M, Takeuchi Y, Kato K. A memory-type holographic polymer dispersed liquid crystal (HPDLC) reflective display device. J. Phys. D. Appl. Phys. 1998;31:2225–2230.

[3] Coates D. Polymer-dispersed Liquid Crystals. J. Mater. Chem. 1995;5:2063–2072.

[4] Drzaic PS. Liquid Crystals Dispersions. Singapore: World Scientific; 1995.

[5] Hoppe CE, Galante MJ, Oyanguren PA, et al. Thermally Reversible Light Scattering Films Based on Droplets of a Liquid Crystal (N -4-Ethoxybenzylidene-4 ′ - n -butylaniline)/ Polystyrene Solution Dispersed in an Epoxy Matrix. Macromolecules. 2004;37:5352–5357.

[6] Hoppe CE, Galante MJ, Oyanguren PA, et al. Polymer-Dispersed Liquid Crystals with Co-continuous Structures Generated by Polymerization-Induced Phase Separation of EBBA-Epoxy Solutions. Macromolecules. 2002;35:6324–6331.

[7] Smith GW. Cure Parameters and Phase Behavior of An Ultraviolet-Cured Polymer- Dispersed Liquid Crystal. Mol. Cryst. Liq. Cryst. 1991;196:89–102.

[8] Amundson K, Blaaderen A Van, Wiltzius P. Morphology and electro-optic properties of polymer-dispersed liquid-crystal films. Phys. Rev. E. 1997;55:1646–1654.

[9] Marin L, Popescu MC, Zabulica A, et al. Chitosan as matrix for bio-polymer dispersed liquid crystal systems. Carbohydr. Polym. 2013;95:16–24.

[10] Marin L, Ailincai D, Paslaru E. Monodisperse PDLC composites generated by use of polyvinyl alcohol boric acid as matrix. RSC Adv. 2014;4:38397.

[11] Ailincai D, Farcau C, Paslaru E, et al. PDLC composites based on polyvinyl boric acid matrix – a promising pathway towards biomedical engineering. Liq. Cryst. 2016;43:1973–1985.

[12] Perju E, Paslaru E, Marin L. Polymer-dispersed liquid crystal composites for bio-applications: thermotropic, surface and optical properties. Liq. Cryst. 2015;42:370–382.

[13] Aouada FA, De Moura MR, Fernandes PRG, et al. Optical and morphological characterization of polyacrylamide hydrogel and liquid crystal systems. Eur. Polym. J. 2005;41:2134–2141.

[14] Hsu T-CC, Lu C-HH, Huang YY-T, et al. Concentric polymer-dispersed liquid crystal rings for light intensity modulation. Sensors Actuators A Phys. 2011;169:341–346.

[15] Nakabayashi N, Takarada K. Effect of HEMA on bonding to dentin. Dent. Mater.

1992;8:125–130.

[16] Park J, Ye Q, Topp EM, et al. Effect of photoinitiator system and water content on dynamic mechanical properties of a light-cured bisGMA/HEMA dental resin. J. Biomed. Mater. Res. A. 2010;93:1245–1251.

[17] Montheard J, Chatzopoulos M, Chappard D. 2-Hydroxyethyl Methacrylate (HEMA): Chemical Properties and Applications in Biomedical Fields. J. Macromol. Sci. Part C. 1992;32:1–34.

[18] Pedley DG, Skelly PJ, Tighe BJ. Hydrogels in Biomedical Applications. Br. Polym. J. 1980;12:99–110.

[19] Pimenta AFR, Ascenso J, Fernandes JCS, et al. Controlled drug release from hydrogels for contact lenses: Drug partitioning and diffusion. Int. J. Pharm. 2016;515:467–475.

[20] Courten C De, Bucher PJM, Benezra D. Experience with HEMA Lenses in Paediatric Cataract. Eur. J. Implant Refract. Surg. 1990;2:315–318.

[21] Bellucci R. An Introduction to Intraocular Lenses: Material, Optics, Haptics, Design and Aberration. In: J.L. G, editor. Cataract ESASO Course Ser. vol 3. Basel: Krager; 2013. p. 38–55.

[22] Goodner MD, Lee HR, Bowman CN. Method for Determining the Kinetic Parameters in Diffusion-Controlled Free-Radical Homopolymerizations. Ind. Eng. Chem. Res. 1997;36:1247–1252.

[23] Yilmaz L, Mchugh a J. Analysis of Nonsolvent -Solvent -Polymer Phase Diagrams and Their Relevance to Membrane Formation Modeling. J. Appl.

Polym. Sci. 1986;31:997–1018.

[24] Altena FW, Smolders C a. Calculation of liquid-liquid phase separation in a ternary system of a polymer in a mixture of a solvent and a nonsolvent. Macromolecules. 1982;15:1491–1497.

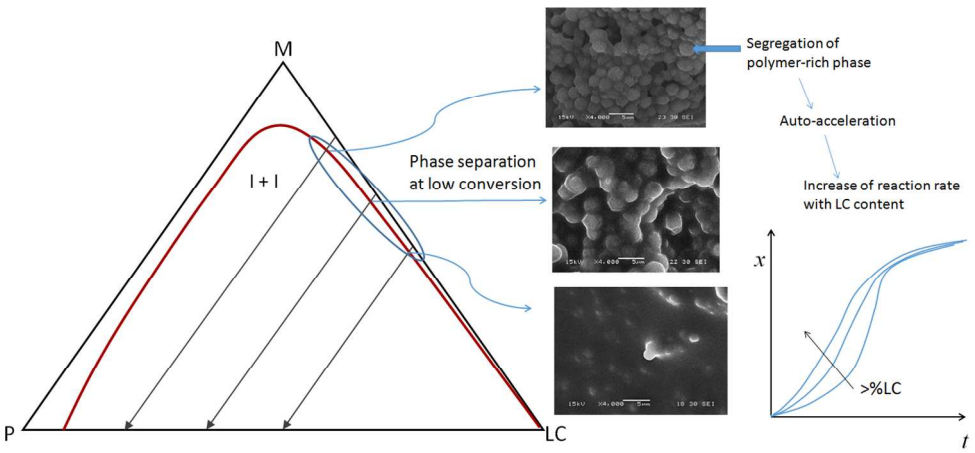

402x180mm (96 x 96 DPI)

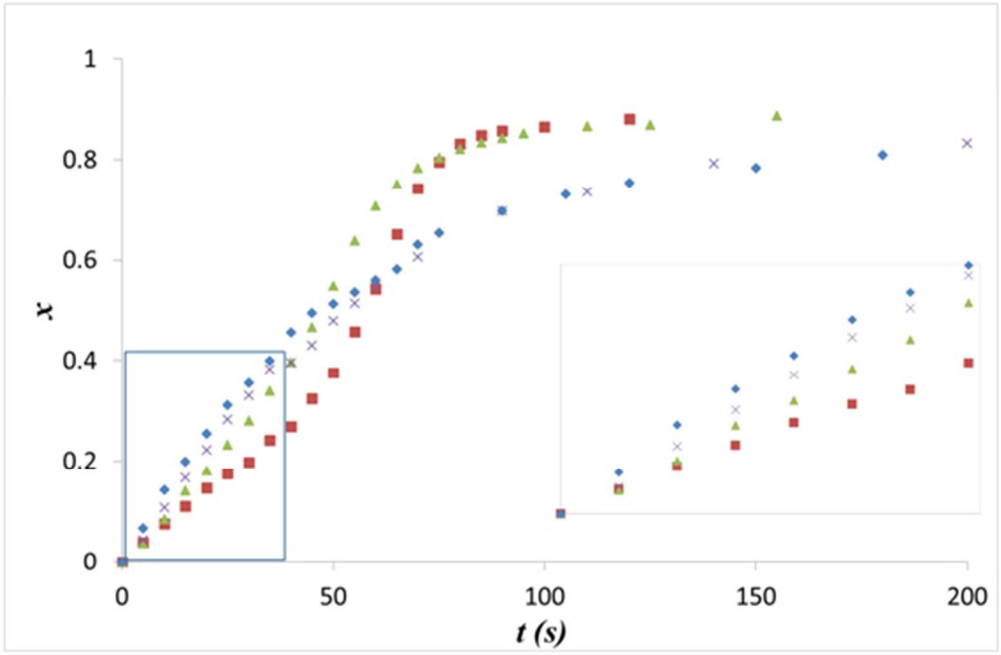

Figure 1. Polymerization kinetics of HEMA with different %wt contents of 8CB: 0 (squares), 15 (triangles), 30 (crosses) and 50 (diamonds). The inset shows the low-conversion region.

151x98mm (96 x 96 DPI)

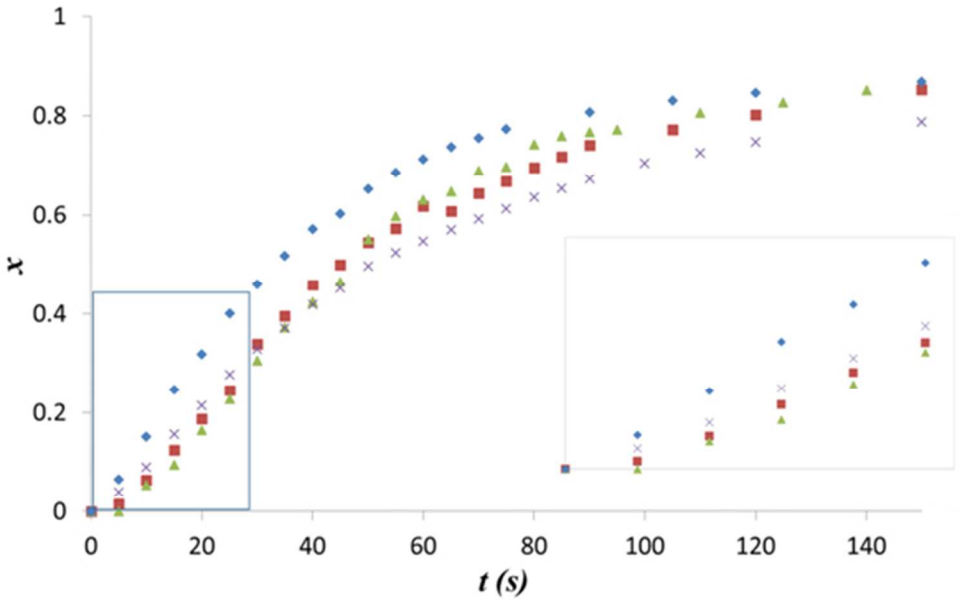

Figure 2. Polymerization kinetics of materials with 50%wt of LC: HEMA/5CB (diamonds), HEMA/8CB (crosses), HPMA/5CB (squares), HPMA/8CB (triangles). The inset shows the low-conversion region.

160x103mm (96 x 96 DPI)

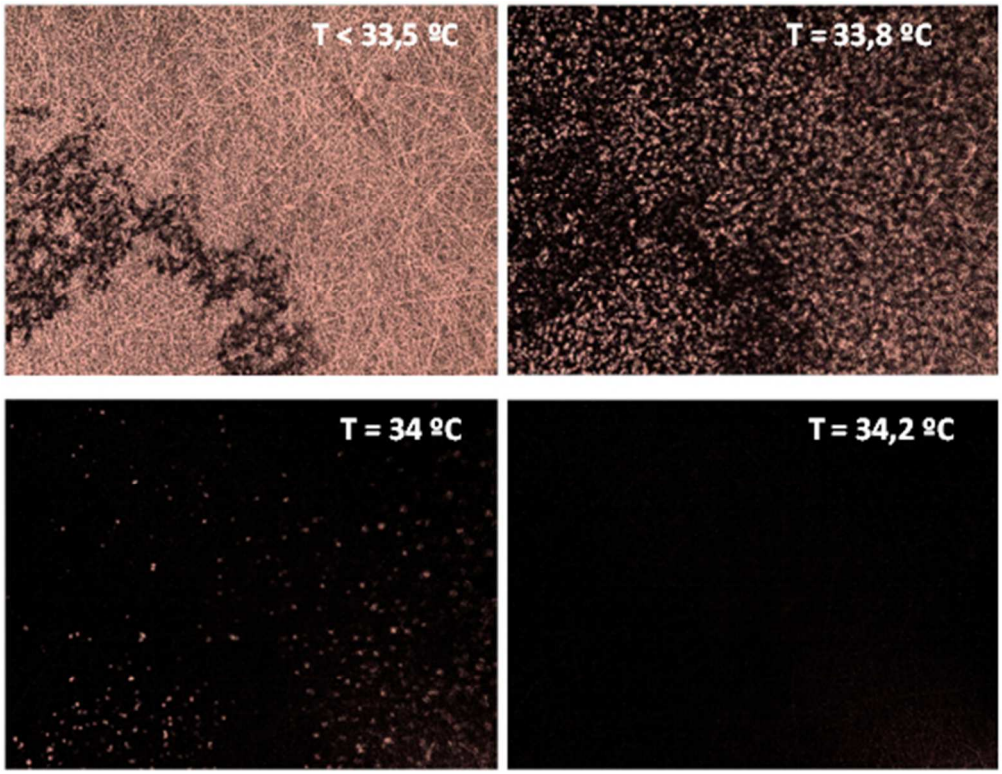

Figure 3. POM micrographs of PHEMA/8CB-30 at different temperatures (as indicated). Each micrography is an area of about 1mm x 1mm.

142x110mm (96 x 96 DPI)

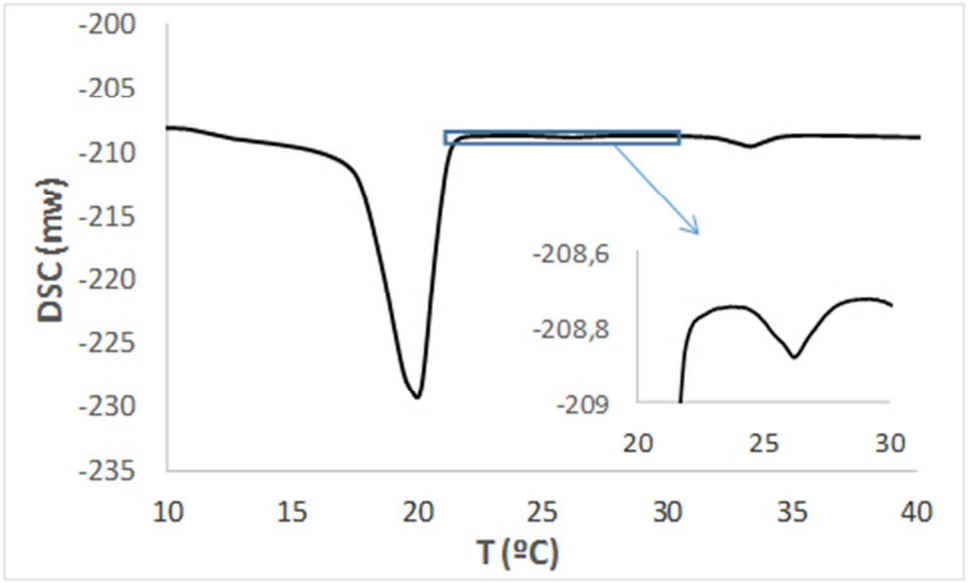

Figure 4. DSC thermogram of PHEMA/8CB-30. The inset shows a zoom into the smectic-nematic transition.

128x77mm (96 x 96 DPI)

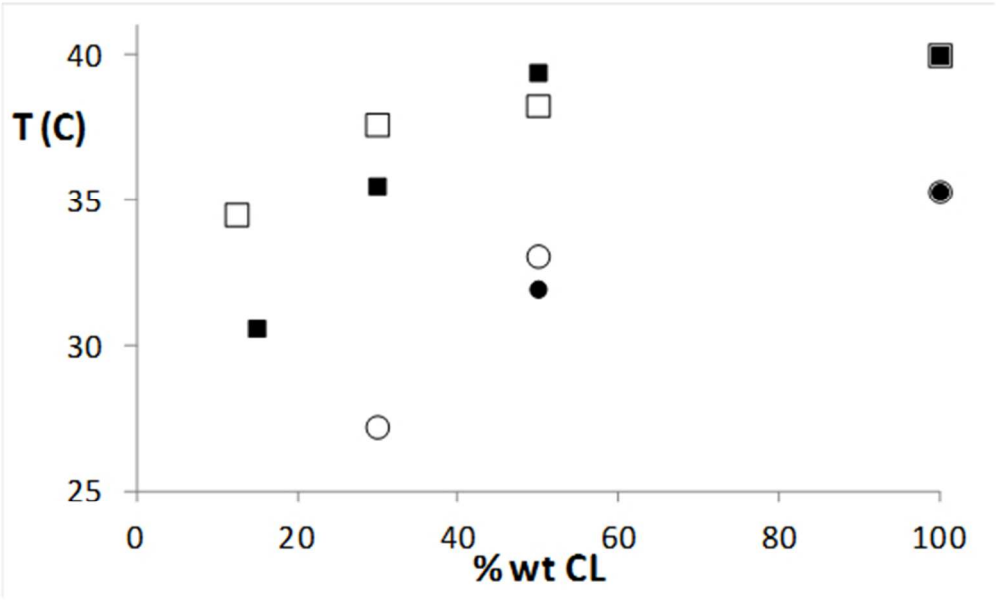

Figure 5. TNI,∞ for different materials. The following code is used: squares for 8CB, cyrcles for 5CB, empty symbols for HPMA, full symbols for HEMA.

146x88mm (96 x 96 DPI)

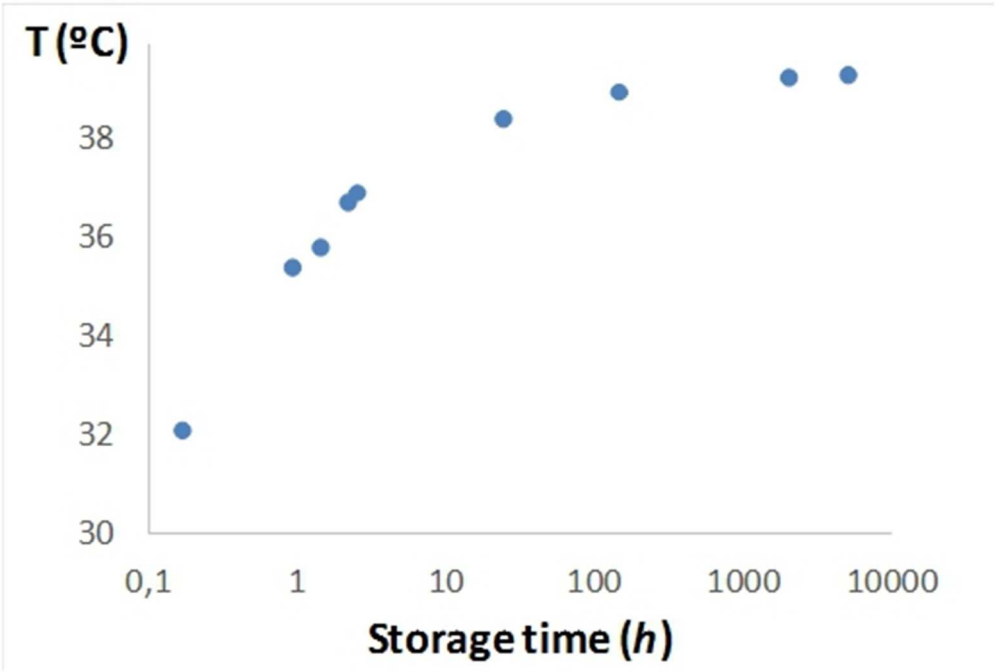

Figure 6. TNI as a function of storage time (in dark), after 15 minutes of irradiation, for PHEMA/8CB-50 (note that time scale is logarithmic).

136x92mm (96 x 96 DPI)

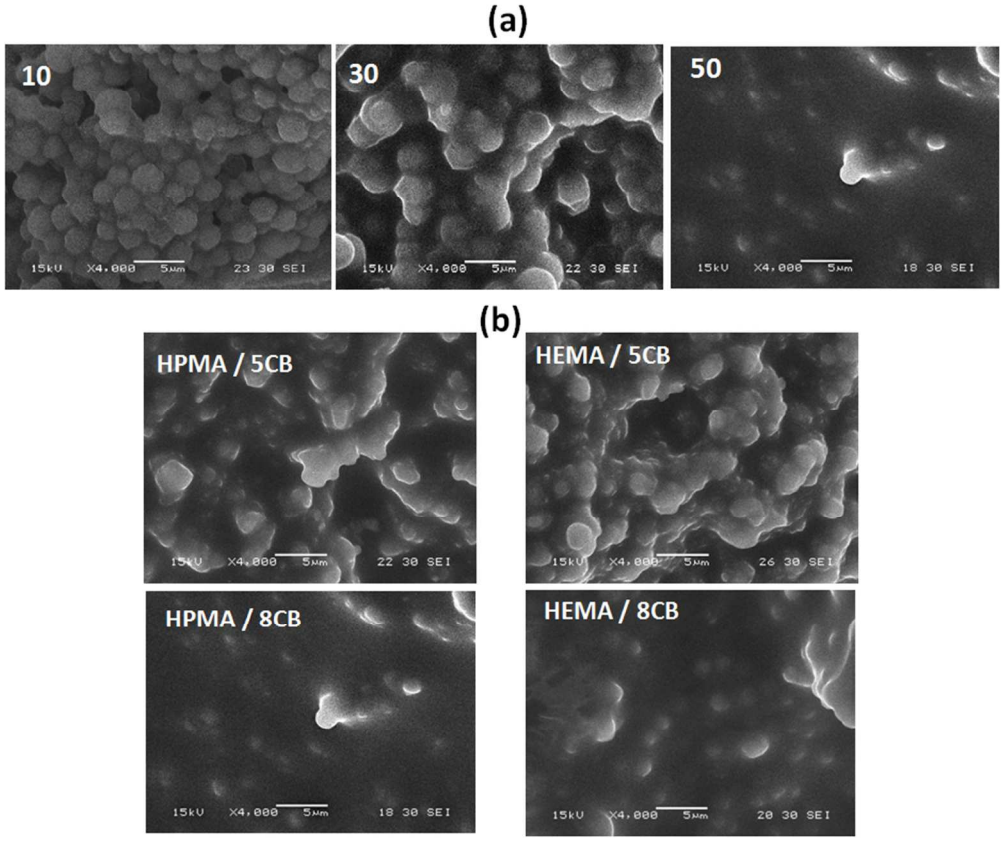

Figure 7. SEM micrographs of different materials at full conversion. (a) HPMA / 8CB, with different amounts of LC (as indicated in each micrograph). (b) different combinations of matrices and LCs (indicated in each micrographs), LC content 50%wt.

248x211mm (96 x 96 DPI)

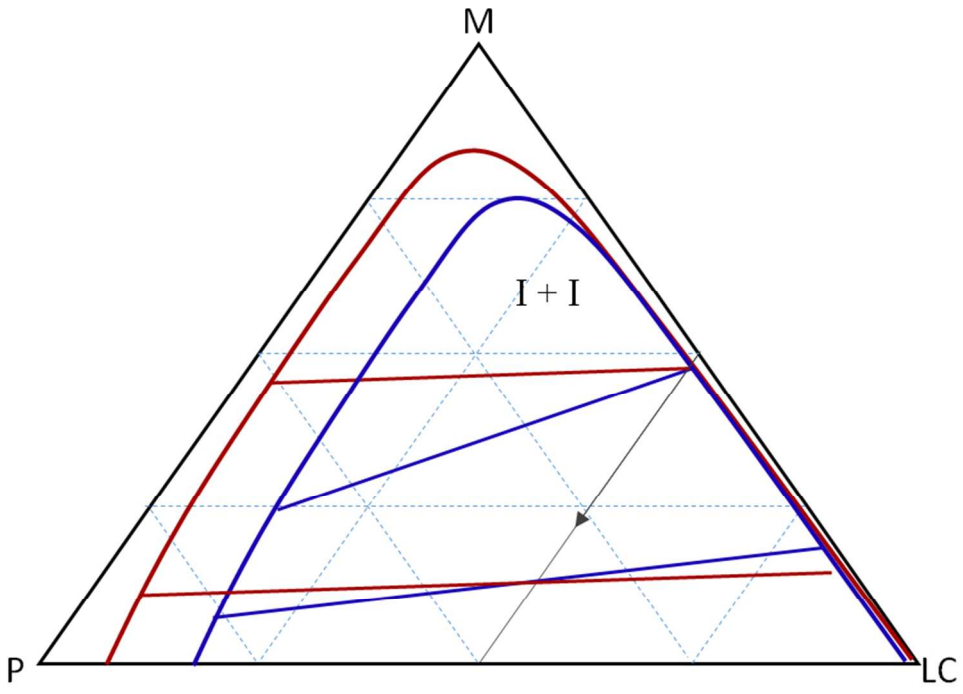

Figure 8. Schematic of the qualitaive ternary phase diagrams, showing only the difference between LCs: 8CB is represented in red and 5CB in blue. Each vertex is a pure component, monomer (M), polymer (P) and LC. Only I-I phase coexistence is shown, as the nematic phase is expected to be confined in a very narrow region close to the LC vertix. The dotted lines are lines of constant composition of one component. The full gray line with an arrow indicates the trajectory of a reacting system (aprox. 50% LC) as conversion increases.

237x170mm (96 x 96 DPI)